The Scattering and Absorption Effects of Fluorescence Spectroscopy in a Real Time Optical Biopsy

Seunghee Han*†, Markus G. Müller*, Seunghee Kang†§, Haejin Kang‖

*G.R.Harrison Spectroscopy Lab, Massachusetts Institute of Technology**

Department of System Engineering †,Radiation Oncology †, Radiology §,

Ajou University, Suwon, Kyungkido

The fluorescence emanating from a biological tissue contains information about scattering, absorption and the intrinsic fluorescence (fluorescence only due to fluorophores). Becaue fluorescence spectra of biological tissue are often significantly affected by the presence of tissue absorbers and scatterers, the measured tissue fluorescence cannot be interpreted as a linear combination of intrinsic fluorescence spectra of different tissue biochemical. We conducted experiments to examine the influence of scattering and absorption on the experimentally measured fluorescence of a turbid medium such as biological tissue. Therefore, we acquired fluorescence and reflectance spectra of tissue phantoms with a wide range of scatterer and absorber concentrations. By applying a photon migration model, which uses the scattering and absorption information contained in reflectance spectra to remove their distortion also present in fluorescence spectra, we extract the intrinsic fluorescence of these tissue models. We achieved excellent agreement between modeled and actual intrinsic fluorescence spectra. The motivation for this research is that intrinsic fluorescence spectra are expected to change with progression of disease in human tissue, due to changes in the tissue biochemical composition. It is not possible to distinguish the two tissue types by using only the measured fluorescence, however clear separation can be achieved with the intrinsic fluorescence in real time optical biopsy.

Key Words: Optical Biopsy, Intrinsic Fluorescence, Absorption, Scattering.

Introduction

Optical spectroscopy techniques have in recent years been investigated in the search for novel, minimally or non-invasive methods for tissue characterization and for measurements of various parameters in the tissue. The techniques developed for tissue characterization are frequently called "optical biopsy"[1], a term that is somewhat contradictory, since the term biopsy refers to the removal of tissue, while the word optical implies that tissue is not removed. Spectroscopy has the advantage of being fast, easy to implement and very sensitive to small changes in the fluorescence lineshape and intensity. The goal is to detect small alterations in real time in the biochemical composition or morphological structure in the development of diseases inside the tissue

§Corresponding author

before it progresses further. Progressed stages of diseased tissue can be visible by eye (*e.g.* with the endoscope) but progressed disease complicates or sometimes even makes treatment impossible (*e.g.* cancer). Currently, there is no sensitive diagnostic instrument for precancerous (dysplastic) lesions *in vivo*. In general a physician visually examines tissue and takes biopsies, often random, from suspicious sites. Other diagnostic techniques like nuclear magnetic resonance imaging does not usually provide information about small lesions, only larger tumors are sometimes detectable due to changes in their morphology *e.g.* large vasculature. The same problem with bad resolution exists in X-ray computer tomography.

Besides the insufficient sensitivity /resolution to detect tissue alterations, these systems are very expensive. It is also important to note that more than 85% of all cancers originate in the epithelium[2] a superficial highly cellular tissue layer. Therefore these cancers are theoretically detectable by fiber based optical systems because of the sufficient penetration depth of light. Hence, large volume probing systems are not needed. Locating and classifying diseased tissue with light inside a living patient is an exciting non invasive alternative to taking tissue biopsy samples, which are examined later under the microscope by a pathologist, the current gold standard in the field.

The problem that arises in fluorescence spectroscopy of human tissue optical biopsy is how to interpret fluorescence or white light reflectance spectra. Fluorescence and reflectance spectra of biological tissue are often significantly affected by the presence of tissue absorbers and scatterers. Therefore, the measured tissue fluorescence cannot be interpreted as a linear combination of intrinsic fluorescence spectra of different tissue biochemicals, where we define intrinsic fluorescence as fluorescence only due to fluorophores without the effects of absorbers and scatterers. The occurrence of the same distortion effects in the fluorescence as in the reflectance spectra shows how closely related both are. This leads us to the educated guess that it is important to understand the physical nature of the diffuse reflection in order to comprehend the fluorescence. A method to express diffuse reflectance with basic optical parameters, the absorption and scattering coefficient, has been previously proposed by Zonios *et al*[3]. Hence, we present a method to obtain the intrinsic fluorescence by using information contained in the corresponding diffuse reflectance spectrum to disentangle the effects of scattering and absorption from the measured fluorescence spectrum. Until now, a simple and reliable method to extract the intrinsic fluorescence of a turbid medium does not exist.

Material and Methods

Tissue scattering and absorption

The tissue optical properties[4] mainly consist of the scattering and absorption properties of the tissue components. From the transport theory point view, the scattering and absorption coefficients, μ_s and μ_a, respectively, are defined as the radiant energy loss per incremental unit photon path length in tissue due to scattering and absortion.

The scattering in tissue due to the random discontinuity in refractive index on the microscopic level, such as the aqueous-lipid membrane interfaces surrounding and within each cell or the collagen fibrils within the extracellular matrix. According to the electrodynamic theory, the scattering cross section, which is related to the scattering coefficient by a density term, is a function of both the wavelength and the size of the scattering particle.

Scattering in tissues is generally strongly forward directed (anisotropic). That means that incoming light does not change its direction much after a scattering event. This is because the wavelength of light is of the same order or smaller than the scatterer. The angular distribution of scattered light is described by the phase function, $p(\theta)$, which gives the probability of a photon being scattered at an angle, θ, respective to the incident direction. The phase function is often approximated by the Henyey-Greenstein phase function[4],

$$p(\theta)=\frac{1}{4\pi}\frac{1-g^2}{\left(1-g^2+2g\cos\theta\right)^{3/2}} \qquad (1)$$

with g being the average cosine of the scattering angle:

$$g=2\pi\int_0^{\pi}p(\theta)\cos\theta\sin\theta d\theta \qquad (2)$$

The value of g is usually between 0.7 and 0.98 for tissue (anisotropic forward scattering) and 0 for the isotropic case. Another often used parameter, the reduced scattering coefficient, μ_s', defined as $\mu_s' = \mu_s (1-g)$, already incorporates the anisotropic effect of *g*. Therefore, the inverse of μ_s' has the meaning of the path length light travels until it is isotropically distributed due to several scattering events. We essentially convert the computations for an anisotropic case into an isotropic one.

The absorption of light in tissue is due to the natural chromophores and is strongly wavelength dependent. Absorption spectra usually show distinct peaks because of the discrete energy levels of the tissue chromophores. In the ultraviolet region, the peptide bonds and amino acids in proteins and purine and pyrimidine bases in nucleic acids absorb strongly. The visible light is absorbed dominantly by some specific chromophores, which contain highly conjugated(double bonds) system, such as hemoglobin, myoglobin, cytochrome pigments, and melanin pigment. At longer wavelength in the infrared, the absorption by tissue water is high. Absorbers usually attenuate light exponentially with Lambert-Beers law[5]. In the wavelength range of this study, 360 nm to 700 nm, hemoglobin is the dominant absorber in the surface mucosa of tissues such as colon, cervix, oral cavity, esophagus *etc.*, which are currently being studied for early cancer diagnosis. The

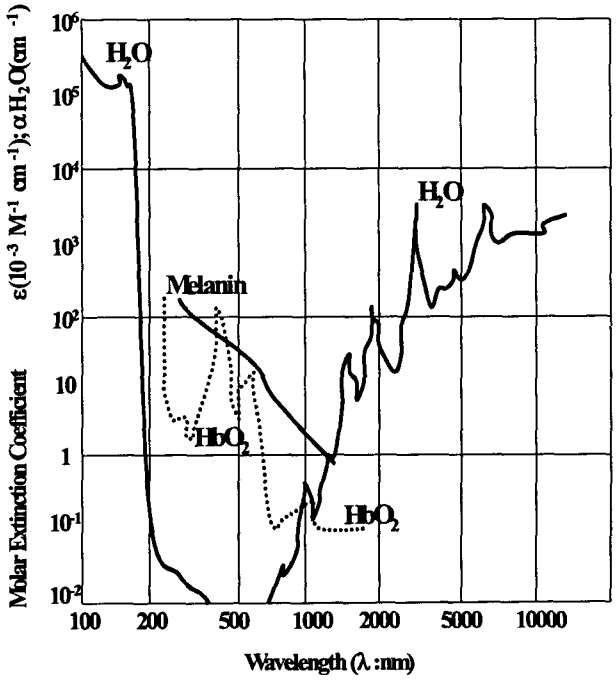

Figure .1: The figure shows absorption spectra of water, oxy-hemoglobin, and melanin. These are typical absorbers in human tissue for a wavelength range from the ultra-violet to the infra-red. Due to low absorption in the diagnostic window around 800 nm light penetration depth of more than a centimeter can be achieved. Water is the major absorber except in the visible, which is of most interest in this study. (From Itzkan. I, Izatt. J. A.)[6]

absorption of water in this range can be neglected, as can be seen in Figure 1. Other light absorbing biochemicals like melanin and β -carotene are only contained in significant amounts in skin and arteries respectively, but not in other tissues. DNA, amino acids and therefore proteins have strong absorption bands, which are generally only important below 300 nm. This indicates that in our case the diffuse reflectance and fluorescence of tissue is mostly affected by scattering and hemoglobin absorption. Hemoglobin absorbs light strongly in the blue, which is responsible for its characteristic red color. Red blood cells contain hemoglobin, they transport oxygen, carbon dioxide, hydrogen ions and carbon monoxide between the alveoli of the lungs and the tissue. Hemoglobin exists in two forms: the oxygenated (HbO_2) and the deoxygenated (Hb). Both have similar absorption spectra (Figure 2).

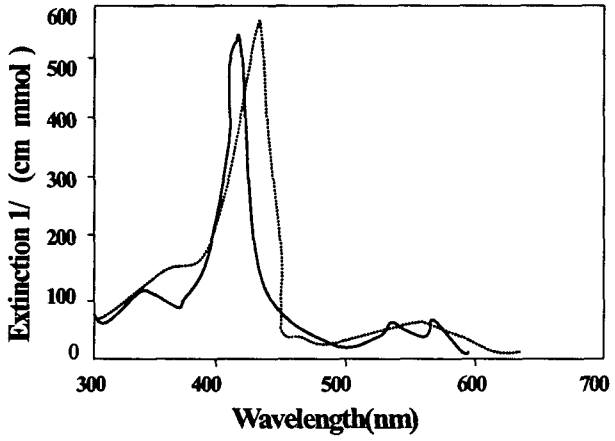

Figure .2: Oxy-hemoglobin(_____) and deoxy- hemoglobin (...)absorption spectra for visible and near-UV wavelength. Note the small differences in the two spectra at 420 nm, 540 nm and 580 nm. (from Prahl. S: Oregon Medical Laser Center website)

When a photon gets absorbed by a molecule/atom, it elevates the chromophore into an excited state by lifting up one of its ground state electrons into a higher energy level without a change in electron spin (Figure 3). Afterwards, the molecule relaxes either non-radiatively or radiatively, depending on its structure. In radiative processes, a photon usually with lower energy than the initial excitation photon is emitted. If no electron spin flip occurs we call the process fluorescence. We call the process phosphorescence in case of an intersystem conversion in which the spin is flipped by crossing over into another excited state and relaxes to the ground state with another spin flip. These typically slow decays are rarer than the fluorescence events.

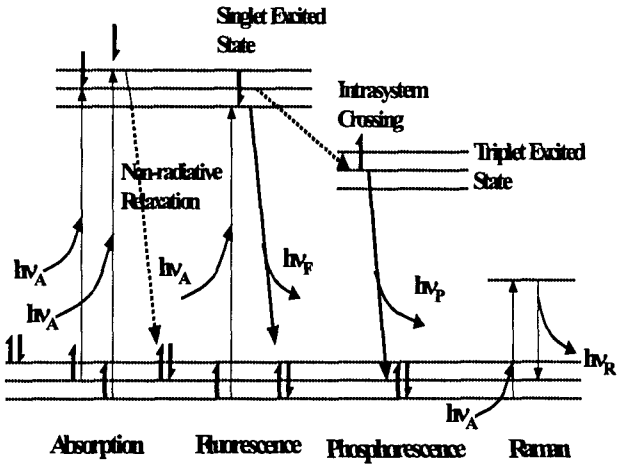

Figure .3: Jablonski diagram detailing the atomic transitions that occur with absorption and with relaxation resulting in fluorescence and phosphorescence. Raman scattering arises from inelastic scattering associated with alterations in the populations of the vibrational energy levels (from Richards-Kortum and Sevick-Muraca)[4]

Photon Migration

In order to extract intrinsic fluorescence from experimentally measured tissue fluorescence and reflectance, Zhang *et al*[7]. extended and refined the photon migration model introduced by Wu *et al*[8].. In this model, light propagation in a turbid medium is described in terms of photons traveling in paths with discrete nodes (or photon-matter interaction events such as absorption, scattering, fluorescence *etc.*). There are two elementary

properties associated with each path: the path probability ρ in the ensemble of all possible paths, and the photon weight w at the end of the path for each photon injected at the beginning of the path. With these quantities, reflectance, R, and fluorescence, F, can be expressed as,

$$R = \sum_{n=1}^{\infty} \rho_n w_n$$
$$F = \sum_{n=1}^{\infty} \sum_{i=0}^{n-1} \rho_{ni} w_{ni} \qquad (3)$$

The subscript n indicates a reflectance path with n nodes while the subscript ni characterizes a fluorescence path with scattering/absorption events of the excitation light during the first i nodes, the conversion of excitation light into fluorescent light at the i+1th node and scattering/absorption of the fluorescence light during the remaining n-i-1 nodes. The following assumptions[7,8] have been made about path probabilities and photon weights for reflectance and fluorescence paths

$$\begin{cases} \rho_n = \alpha e^{-\beta n} & w_n = a^n \\ \rho_{ni} = \sqrt{\alpha_x \alpha_m} e^{-\beta_x (i+1)} e^{-\beta_m (n-i-1)} & w_{ni} = a_x^{i+1} \dfrac{f_{xm}}{\mu_{sx} l} a_m^{n-i-1} \end{cases} \qquad (4)$$

where the subscripts x and m indicate dependence of quantity on excitation and emission wavelengths respectively. The albedo, a, is given by the expression $a = \mu_s/(\mu_a + \mu_s)$ with μ_a and μ_s the absorption and scattering coefficients of the turbid medium, respectively. Letting R_0 be the reflectance in absence of absorption (*i.e.* μ_a =0 or $a=1$) and letting $\delta = e^{\beta} - 1$, we have $a = \delta R_0$. According to Wu *et al*[8]. $\beta = S(1-g)$, where S is a probe specific constant and g is the anisotropy parameter of the medium. The quantity f_{xm} denotes the intrinsic fluorescence intensity and l is a probe geometry dependent constant with a dimension of length. It can be related to the effective depth of fluorescent light collected by the probe.

Using the assumptions in Eq. (4), both the reflectance and fluorescence in Eq. (3) can be evaluated readily. Thus a relationship between fluorescence and reflectance was established[7] from which the intrinsic fluorescence was expressed as

$$f_{xm} = \frac{F_{xm}}{\dfrac{1}{\mu_{sx} l} \sqrt{\dfrac{R_{0x} R_{0m}}{\delta_x \delta_m}} \dfrac{R_x}{R_{0x}} \left(\dfrac{R_m}{R_{0m}} + \delta_m \right)} \qquad (5)$$

Notice that Eq.(5) establishes a relationship between the intrinsic fluorescence spectrum, f_{xm}, and the experimentally measured fluorescence, F_{xm}, and reflectance spectra, R_m.. A simple physical interpretation was offered as follows. When reflectance and fluorescence are collected from a given tissue site with the same probe, absorption and scattering distort fluorescence and reflectance spectra similarly, because the diffusely reflected and fluorescent photons delivered/collected by the probe traverse similar paths. This enables one to exploit the absorption and scattering information contained in the reflectance spectrum to recover the intrinsic, distortion-free fluorescence spectrum. It is interesting to discuss the following three limiting cases;

$R/R_0 >> \delta$: In this case where absorption is weak so that R/R_0 is relatively large compared to δ, Eq. (5) can essentially be reduced to a simple ratio between measured fluorescence and reflectance, thus leading to a dubbed name for the extraction method of "F over R" .

$R/R_0 << \delta$:In this case, Eq. (5) is essentially the same as the measured fluorescence. Thus, the correction is negligible.

R/R_0 =1: In this case, there is no absorption so that R/R_0 is unity by definition and Eq. (5) can be reduced to

$$f_{xm} = \frac{F_{xm}}{\frac{\gamma}{\mu_{sx}}\sqrt{\frac{R_{0x}R_{0m}}{\delta_x\delta_m}(1+\delta_m)}} \qquad (6)$$

Instrument

All reflectance and fluorescence spectra presented in this study are obtained with an improved version of the FastEEM instrument[9]. A xenon flash lamp (EG&G Optoelectronics, FX-139) is used as a white light source to acquire reflectance spectra in the range from 380 nm -700 nm. Excitation light sources for fluorescence measurements are provided by a nitrogen laser (Laser Science, Inc.) (337nm) and ten different dye lasers (358 nm - 610 nm) sequentially pumped by the nitrogen laser. The dye cuvettes are mounted on a rotating wheel driven by a stepper motor. The excitation light is coupled into a fiber bundle with a central excitation fiber surrounded by six collection fibers[10]. At the tip of the probe all seven fibers (200㎛ core diameter) are fused together creating a quartz shield of 1.5 mm diameter which is beveled and then polished at a 17° angle to reduce internal reflections from the boundary between glass and tissue. The fused tip and the fibers are surrounded by silver epoxy (only at the tip) and by Teflon tubing to strengthen the probe. During each measurement the probe tip is brought in contact with the surface of the sample under investigation. Fluorescence and reflectance signals are collected by the six collection fibers of the probe through the same probe tip. A wheel of long pass filters is used to prevent reflected laser excitation light from reaching the spectrograph (CP 200, Jobin Yvon SA) and the intensified diode array detector (EG&G Instruments Princeton Applied Research). Fluorescence spectra at eleven excitation wavelengths and reflectance spectra can be collected in less than one second (Figure 4). The whole system is controlled by a 486X personal computer and spectra are recorded with Oma Vision (EG&G Instruments Princeton Applied Research) software. The wavelength scale and the spectral response of the system are calibrated with a mercury lamp and a NIST standard tungsten lamp, respectively. A concentrated Barium Sulfate (concentration > 20%) suspension is used for reflectance calibration.

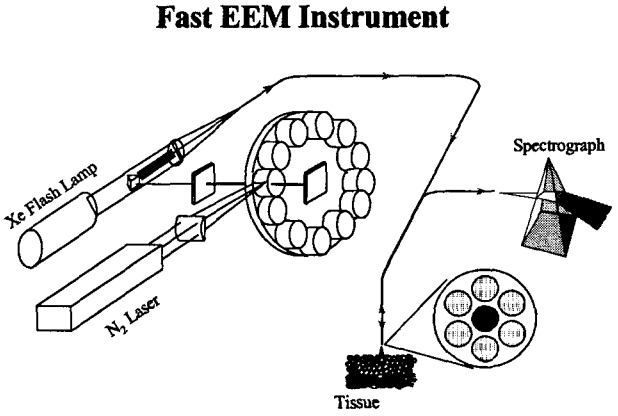

Figure .4: The FastEEM system, with Xe flash lamp, nitrogen laser, dye wheel, fiber optics and spectrograph. The fiber is brought in contact with the tissue and fluorescence and reflectance spectra are obtained in 1 sec. On the right we can see the fiber bundle, six collection fibers around one excitation fiber.

Tissue Phantoms (Furan and Rhodamine dyes)

The tissue phantoms are suspensions of polystyrene microspheres (1 ㎛ diameter, Polybead, Polyscience), a water-soluble dye (Furan 2 Lambdachrome), and ferrous human hemoglobin powder (Sigma) dissolved in deionized water. Hemoglobin is the major absorber in the visible for tissues of interest[3], and Furan 2 fluoresces in the same range as collagen for UV-A excitation. Polystyrene beads are used to simulate the average scattering properties of tissue[3,11]. The fluorescence of polystyrene beads and the scattering from hemoglobin and the fluorophore

molecules are negligible. Additionally, tissue phantoms with Rhodamine B are created in the same way as described above for Furan 2. Rhodamine B is used because of its fluorescence emission in the red wavelength range, since Furan 2 only gives rise to fluorescence in the blue.

The phantom components are mixed in a glass bottle and diluted with deionized water to the concentration of interest. The diameter of the bottle is 1.5 cm, which is about 40 times higher than the transport mean free path, $1/\mu_t'$, at the wavelengths of interest. Thus, edge effects are insignificant. This is further verified by experiments performed on phantoms in larger jars with different boundaries where no difference in fluorescence and reflectance spectra is observed. For the experiments with the Furan 2 dye only excitations at 337 nm and 358 nm result in appreciable fluorescence since the extinction coefficient of the dye (Furan 2) approaches zero at approximately 370 nm[12]. The Rhodamine phantoms on the other hand exhibit fluorescence for all excitation wavelengths.

To make meaningful comparisons between the fluorescence spectra, care has been taken to ensure that the fluorescence in these spectra is only due to the fluorophore in the phantom. The background fluorescence of suspensions containing only beads at the same concentrations as the Furan phantoms is measured and later subtracted from the fluorescence of the corresponding phantoms. This signal is small, less than 5% of the Furan fluorescence signal, and proportional to the bead concentration. We believe that part of this background fluorescence is due to excitation light entering the probe, either after being scattered back by the medium or after being specularly reflected, and creating internal fluorescence in the system by exciting the silver epoxy coating that surrounds the fused tip. Additionally, by recording the background we are able to correct for possible fluorescence of the beads and of the excitation light cut off filters of the FastEEM system.

Results

Scattering effects on fluorescence of tissue phantoms

To investigate the effect of scattering on the intensity and spectral shape of a fluorescence spectrum; we acquire fluorescence spectra for a series of phantoms with different scattering coefficients. The phantoms contain deionized water, Furan 2 (0.9 μM) and 1 ㎛ in diameter polystyrene beads at a concentration between 0 and $4x10^{10}$ beads/ml (~0% - 2% in volume) corresponding to a range of the reduced scattering coefficient μ_s' from 0 to 10 mm^{-1} in the visible spectrum. Spectra at 13 different μ_s' values were obtained with 337 nm and 358 nm excitation and some are shown in Figure 5 - a.

The corresponding white light reflectance spectra are presented in Figure 5 - b. Fluorescence spectra of an aqueous dilute solution of Furan 2 (0.9 ㎛) are recorded at 337 nm and 358 nm excitation wavelengths. The first one is presented in Figure 5-a and will be used as the experimentally measured intrinsic fluorescence for Furan 2 phantoms.

Spectral shape

After normalization of the fluorescence spectra shown in Figure 5 - a to their respective peak intensity, all spectra essentially collapsed to the same lineshape as that of the pure Furan dye (Figure 6-a). Only when we take ratios of the phantom fluorescence spectra to the intrinsic fluorescence, we can observe small line shape changes as a function of wavelength approximately 5% over 200 nm (Figure 6-b).

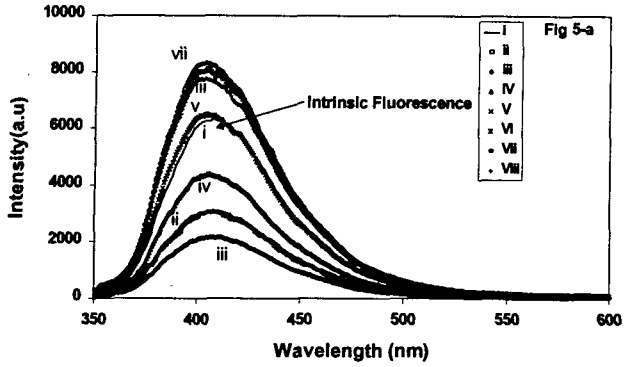

(a)

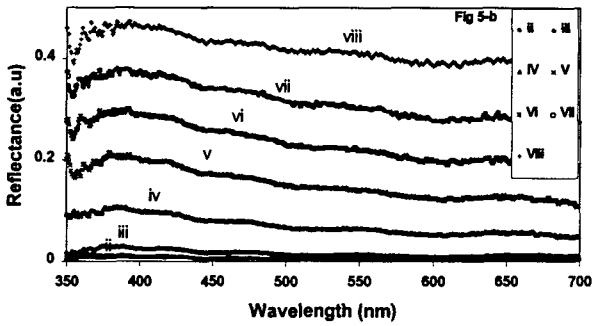

(b)

Figure .5: (5-a) Fluorescence emission spectra (337 nm excitation) and (5-b) corresponding reflectance spectra of physical tissue models, (i) dilute solution of dye (intrinsic fluorescence) and (ii - viii) with various scatterer concentrations (μ s'from 0 to 10 mm-1, a = 0)

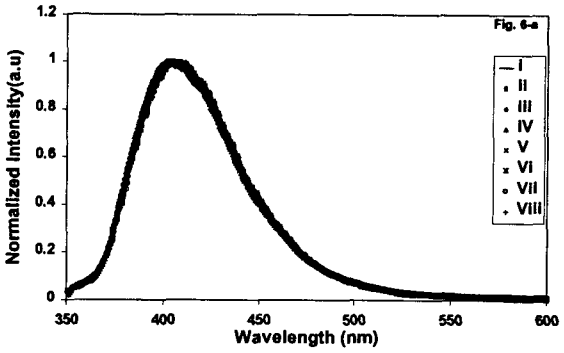

(a)

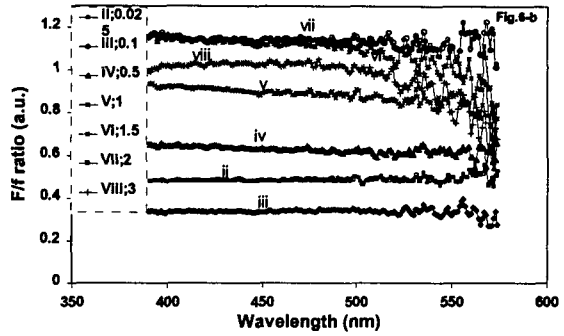

(b)

Figure 6: (6-a) Fluorescence emission spectra of Fig. 5-a normalized to their peak heights; (6-b) fluorescence ratio spectra, normalized to the fluorescence spectrum of the dilute solution of dye of Fig. 5-a. Note the small line shape differences between the intrinsic fluorescence and the fluorescence with scatterers present.

Thus the experiments suggest that scattering has a negligible effect on the fluorescence lineshape. These results are in agreement with Monte Carlo simulations of fluorescence from a highly scattering medium with very small absorption ($\mu_a \approx 0.01\ \mu_s'$) collected by a finite-size probe with a collection angle of 12°. Interestingly, the photon migration model Equation (6) also predicts a similar fluorescence spectral ratio (Figure 7)[8], however fails to describe the correct behavior in the near UV.

Concentration dependence

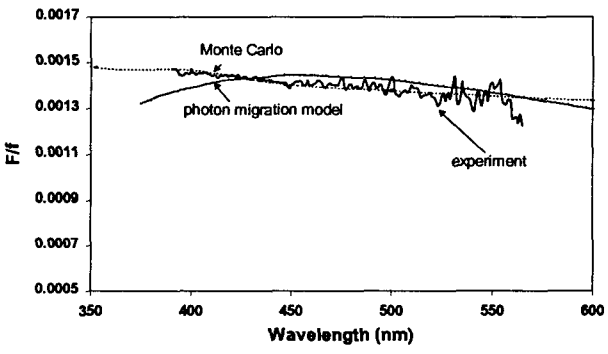

Figure 7. Modeled (theoretical) prediction, Monte-Carlo simulation[8] and experiment (Figure 6-b) of the ratio between the fluorescence of a phantom with a medium scatterer concentration (0.65 % polystyrene beads by volume) and the intrinsic fluorescence. (337 nm excitation).

Fluorescence intensity variations (Furan)

In contrast to the negligible effect of scattering on the fluorescence lineshape, we find that the fluorescence intensity varies with scatterer concentration in a peculiar manner. A representative scatterer concentration dependence of fluorescence intensity is illustrated in Figure 8.

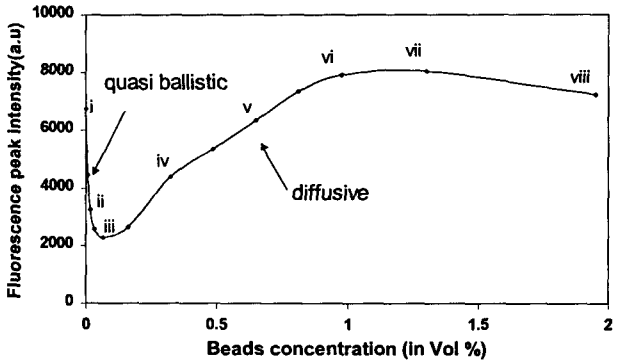

Figure 8. Fluorescence intensity maximum potted as a function of the scatterer concentration for several phantoms with different scatterer concentration (337 nm excitation). Diffusion theory calculated points show the same general trend as the experiment.

The peak position of several fluorescence spectra is plotted against the scatter concentration. It is important to emphasis that the fluorescence intensity is substantially affected by the excitation light distribution, which is dependent on the scatterer concentration of the medium because the detected fluorescence strongly depends on the fluorescence location given through the mean free path of the excitation light. Initially, the fluorescence intensity decreases nearly exponentially, since photons in such tenuous media behave quasi-ballistically. The mean free path is relatively large in such media and therefore fluorescent light is attenuated according to Beers law and reaches the probe without being scattered multiple times. After adding a certain amount of scatterers the fluorescence intensity is increasing again, we approach the diffusion regime.

The observed effects can be understood as follows. As μ_s' increases both excitation and emission light get scattered more and for a scatterer concentration with a mean free path (mfp = $1/\mu_s'$) less than 4 mm, the second region of the curve is entered and we start collecting diffusive light. In this case, the fluorescence intensity increases with the concentration of scatterers. The excitation light cone, which is present in the quasi-ballistic region, is now broadened due to multiple scattering and the mean free paths of the excitation and emission light decreases confining the light in the vicinity of the probe. Therefore, more fluorescent light is collected by the probe, leading to a higher fluorescence intensity. For even higher concentrations of beads, there are two competing effects. On the one hand, the medium becomes even denser and more photons turn back into the probe due to an increase in reflectivity, but on the other hand, the excitation light reaches a smaller amount of dye molecules. Equation (6) describes the fluorescence intensity variations in the diffusion regime quite well, however fails to explain the exponential decrease because the reflectance in Equation (6) approaches zero for decreasing scatter concentrations (not shown).

Fluorescence intensity variations (Rhodamine)

Interesting results are also obtained with Rhodamine phantoms. Note that the minimum of the curve in Figure 9 occurs at $\mu_a \approx \mu_s'$, as before in the case of the Furan dye. That means that by increasing the absorption, the minimum can be shifted to the right, this particular effect has been observed when we added hemoglobin in one of the samples. This effect can also be seen if we use a higher concentrated Rhodamine solution, because Rhodamine absorbs light in the same range it fluoresces as shown in Figure 9.

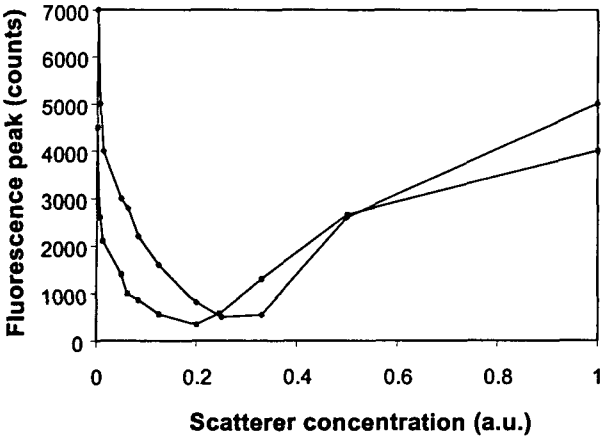

Figure 9. Fluorescence intensity maximum plotted as a function of the scatterer concentration for two phantoms with different Rhodamine concentrations. Due to the higher dye concentration and therefore absorption one of the curves approaches the diffusion regime later.

In addition to the similar intensity variation seen above, we notice a shift in the fluorescence spectrum peak position depending on the scattering concentration. In the quasi-ballistic region the spectral peak position stays constant at about 595 nm however, shifts to the right after traversing the intermediate scattering region (dip) and stays constant again at about 605 nm. This effect can be explained with the help of the Rhodamine absorption spectrum. Although, we use a dilute solution of Rhodamine with a small optical density (absorption coefficient multiplied by the absorption length) and without any scatterers present, reabsorption is observed if we increase the scatter concentration. The fluorophore reabsorbs its own fluorescence light and remits it again at a slightly higher wavelength; this effect shifts the total fluorescence peak to the right. We can conclude that the addition of scatterers increases the effective absorption length in the sample and therefore we can not consider the solution dilute anymore and the peak position of the fluorescence spectrum shifts.

Scattering and absorption effects on fluorescence of tissue phantom

To investigate how absorption affects fluorescence in the presence of scattering, we conduct another set of fluorescence phantom experiments. The phantoms contain the same concentration of beads (0.65% in Volume) with a μ_s' of approximately 2 mm^{-1} and Furan 2 (0.9 μ M) but a varying amount of hemoglobin to change the absorption properties of the medium. The concentration of hemoglobin is varied over a wide range from 0 - 2 g/l, which includes the range of that for most human tissues[13].

In Figure 10-a we present fluorescence spectra for ten phantoms. Decrease in fluorescence intensity and changes in the fluorescence lineshape are evident, as the hemoglobin concentration is increased. To illustrate more clearly the effects of increasing hemoglobin concentration we show in Figure 10-b normalized fluorescence spectra of the intrinsic fluorescence and a phantom with 2 g/l hemoglobin concentration. The characteristic oxy-hemoglobin absorption features are clearly visible in the fluorescence and in the corresponding reflectance spectra shown in Figure 10-a, 10-b and 10-c. The oxy-hemoglobin absorption peaks at approximately 415 nm, 540 nm and 580 nm are seen as dips in the reflectance spectrum and at 415 nm in the fluorescence spectrum.

With the knowledge of the hemoglobin concentrations of the phantoms, one can readily evaluate their absorption coefficients based on documented values of the extinction coefficients for oxy and deoxy hemoglobin[14]. The absorption coefficient corresponding to the hemoglobin concentration turns out to be bellow or of the same order (at 415 nm) as the reduced scattering coefficient (with μ_s' between 2 - 3 mm^{-1}).

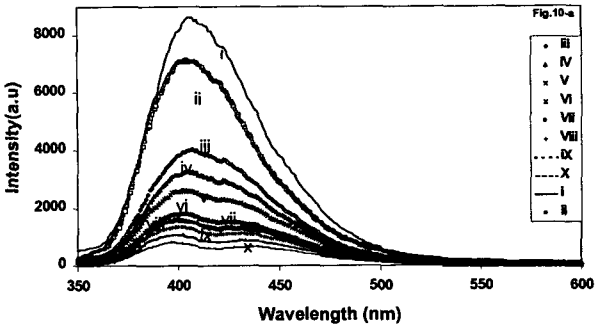

(a)

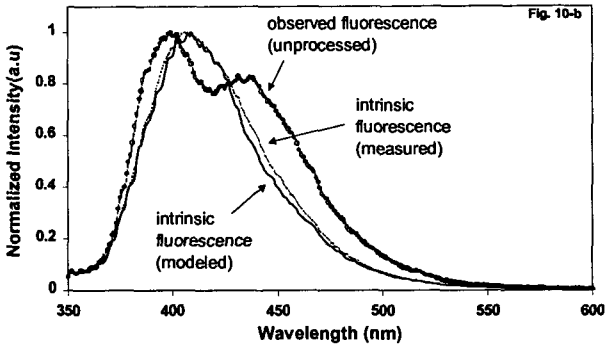

(b)

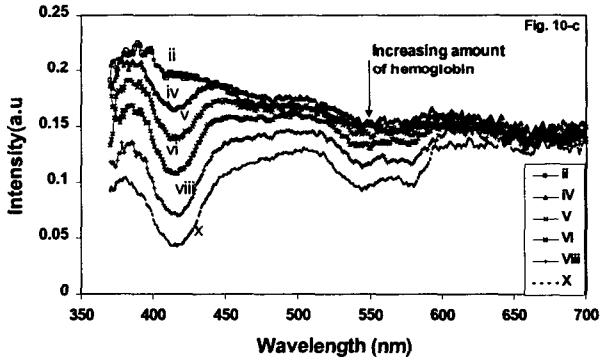

(c)

Figure 10. Effects of absorption/scattering on observed fluorescence. (10-a) Fluorescence spectrum of a dilute solution of dye (i) (intrinsic fluorescence) and physical tissue models with different concentrations of hemoglobin added (i - x); (10-b) comparison of measured and modeled intrinsic fluorescence and observed fluorescence of a sample (Fig. 10-a, ix) with hemoglobin (2 g/l), all spectra are normalized. (10-c) Reflectance spectra of physical tissue models with various absorber concentrations from 0 - 2 g/l. Note the intensity decreases in (10-a) and (10-c) with increasing hemoglobin, especially at the major oxy-hemoglobin absorption peak (415 nm). In all of the above data, μ s was held constant at approximately 1.5 mm-1.

Since the hemoglobin solution is used under ambient conditions (partial oxygen pressure 154 mmHg and room temperature) at pH 7, the hemoglobin is mostly in its oxy-hemoglobin form. Note that the absorption coefficient of Furan 2 is negligible compared to that of hemoglobin. The scattering properties, *i.e.* scattering cross section, σ_s, and anisotropy parameter, g of the polystyrene beads can be calculated using Mie scattering theory[15, 16] because the diameter and refractive index of the beads are known. Thus the known beads number density (1.25 x 10^7 mm^{-3}) allows the reduced scattering coefficient, μ_s' to be evaluated readily. The parameter δ is only dependent on g and the probe specific parameter, S of Equation(5). The value of S is determined once by fitting a fluorescence spectrum of a phantom with known optical properties to the intrinsic fluorescence spectrum using Equation (5). Using this procedure, we find that S is approximately 1 for our system, and S is then fixed to this value during the analysis of the rest of the spectra presented here. The values for R_x and R_{0x} in Equation (5) in the UV ($\lambda < 360$ nm), where the light intensity of the Xe flash lamp is weak and the reflectance signal is noisy, can be obtained by extrapolation of the reflectance spectrum. This can be accomplish with the additional information of the scattering behavior and the hemoglobin absorption spectrum in the UV thereby the reflectance at 337 nm can be recovered very well. Another way to obtain the values of R_x and R_{0x} would be to use the optical parameters μ_s' and μ_a obtained previously and model the diffuse reflectance using a diffuse reflectance model for example the one proposed by Zonios *et al.*[3, 17] . All the other variables F_{xm}, R_m, R_{0m} and R_x for wavelength above 360 nm are obtained experimentally.

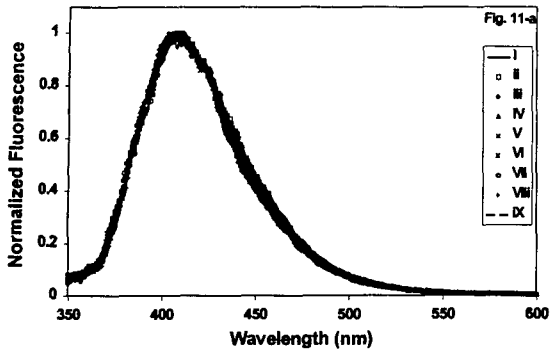

(a)

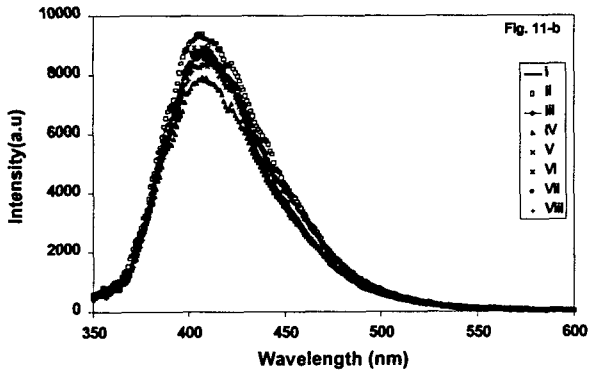

(b)

Figure 11. Intrinsic fluorescence emission spectra, extracted (modeled) from turbid physical tissue models Fig. 10-a, x = 337 nm; (11-a) normalized; (11-b) unnormalized. The measured intrinsic fluorescence is indicated. Note in (11-a) the excellent agreement of the corrected line shapes. The intensity differences in (11-b) are small indicating good intensity corrections of data varying in intensity by up to 450% (compare Fig. 10-a. Analysis of the data gives l = 220㎛.

With the values of the above determined model parameters and the experimentally measured fluorescence and reflectance spectra, we can extract the intrinsic phantom fluorescence (Figure 11-a) by using our photon migration model Equation (5) . Very good agreement between the modeled and the actual intrinsic fluorescence is found for all spectra with different hemoglobin concentration and the hemoglobin absorption dips vanished. Not only we obtain the lineshape of the intrinsic fluorescence, but we also recover the fluorescence intensity information up to a constant scaling parameter l with an accuracy of more than 90% (Figure 11-b). The value for l is found to be approximately 220 ㎛ for the probe used and is obtained by comparing the modeled intrinsic fluorescence intensity with the experimentally measured fluorescence of a dilute dye solution of the same fluorophore concentration.

The intrinsic fluorescence of the Furan 2 dye is obtained at two excitation wavelengths: 337 nm and 358 nm. The two peaks observed in the 400 nm region in the measured fluorescence at 337 nm excitation give rise to a single fluorescence peak in the modeled intrinsic fluorescence. The decreased peak intensity observed in the measured fluorescence with increasing hemoglobin concentration is also removed and the same intrinsic fluorescence lineshape and intensity is recovered for phantoms with the same fluorophore content but varying hemoglobin concentrations.

Additionally, experiments with fixed hemoglobin content and varying beads concentration (0.3% - 0.8% in Volume) have also been performed and have resulted in equally good agreement with the modeled and the actual intrinsic fluorescence.

Discussion

Experiments have been performed to assess the influence of scattering and absorption properties of a medium on the fluorescence intensity and lineshape collected at its surface. To obtain the undistorted intrinsic fluorescence, we have presented a model, which extracts the intrinsic fluorescence of a turbid medium using the measured fluorescence and diffuse reflectance spectra. The model takes advantage of the fact that scattering and absorption affects fluorescence and reflectance in a similar manner. Therefore, diffuse reflectance is used to remove distortions introduced by scattering and absorption from the measured fluorescence. We show that this is possible by expressing the intrinsic fluorescence as a function Equation (5) of measured

fluorescence and reflectance. When comparing this modeled intrinsic fluorescence to the experimentally obtained intrinsic fluorescence very good agreement between model and experiment is obtained. Previous studies performed in the 500 nm range fail to show major lineshape correction[18] and recovering of the intensity[19] or they give only rough approximations of the intrinsic fluorescence.

As mentioned above, the model exploits the similarity between fluorescence path and reflectance path. This similarity enables us to express the first as a function of the second. By looking closely at this assumption we can see that fluorescence which has a narrower wavelength emission range (FWHM < 150 nm) will not be as much affected by the scatterers as reflectance, which is being collected over a much larger range. Fluorescence is created in the medium at a certain depth when the fluorophore absorbs excitation light and remits it isotropically. Therefore, these photons will just travel half the path of the white light reflectance photons which enter the medium with a strong forward direction and have to scatter multiple times in order to turn around back into the probe to be collected. But since the width of the fluorescence lineshape is small and the actual event of the fluorescence takes place inside the medium, the scattering effect on fluorescence is small compared to the reflectance. The fact that fluorescence is isotropic and not anisotropic like the diffuse reflectance, will shorten the total fluorescence pathlength. Another difference between fluorescence and reflectance is that the anisotropy parameter g is not the same for the excitation and the emission path, which will also result in a change of the total pathlength. These effects are partly taken into account in the derivation of Equation (5) by β_1 and β_2, but do not play a important role as long as absorption by the fluorophore is much smaller than scattering and absorption due to hemoglobin. Then, the dye absorption possibility is small and the isotropic effect averages out over the whole photon path.

To discuss Equation (5) in further detail, note that by definition R_0 denotes reflectance in the absence of absorption while R in the presence of absorption. Therefore, the ratio R/R_0 contains information about absorption. The factor R_x/R_{0x} in Equation (5) accounts for effects due to absorption of the excitation photons. When the excitation light gets absorbed inside a turbid medium, its intensity distribution in the medium decreases. This leads to less excitation of fluorophores and thus results in weaker fluorescence emission. The ratio R_x/R_{0x} describes to a large extent the portion of the excitation light that is not absorbed and, therefore, left for generating fluorescent light. Similarly, R_m/R_{0m} accounts for effects due to absorption of the fluorescence photons.

One should note that the model is independent of the absorber, it shows also good results in arterial tissue with varying absorption of beta-carotene. As long as absorption affects fluorescence and reflectance in the same way the model can be used. One limitation however exists in multiple reabsorption and reemission as discussed in the case of Rhodamine B. Without the presence of scattering, a sample of Rhodamine B (4μM) and O.D. < 0.1 would be considered as an optically thin medium. However, we have seen that by adding scatterers in the sample and keeping the Rhodamine B at the same concentration as before we observe fluorescence and absorption of the dye in the reflectance spectra and reabsorption of fluorescence and reemission at a slightly higher wavelength in fluorescence. This observation highlights the interplay between absorption, scattering and fluorescence in a turbid medium. The presence of scattering leads to longer excitation and emission photon paths. Thus, the medium may not be

considered as optically thin in this case and the reabsorption and reemission are not negligible anymore. Also rhodamine absorption at the excitation wavelength is smaller or comparable to the dye absorption at its emission wavelength. These effects are especially apparent for fluorophores with high fluorescence quantum efficiency, small Stokes shift absorption and overlapping emission bands. These factors add more complexity to the problem of recovering the intrinsic fluorescence of a dye like Rhodamine. Since endogenous tissue fluorophores usually have larger Stokes shifts and smaller quantum yields these problems do not arise in tissue. However, in the case of labeling tissue with exogenous dyes reabsorption and reemission might have to be taken into consideration. Another limitations of the model are cases with very high absorber concentrations where the intensity of the diffuse reflectance is strongly decreased and absorption effects become non-linear.

Conclusions

We have analyzed several aspect of light propagation in turbid media to obtain a better understanding of the affect of scattering and absorption in fluorescence and reflectance spectra, which can occur in tissue diagnoses. We have presented a method to express the intrinsic fluorescence with parameters, which are all known through measurements or can be obtained *in vitro* or *in vivo* through calculation/modeling without biopsying the tissue. Since no time intensive calculations like Monte Carlo simulations are involved, the results can be obtained in real time. This enables us to do real time observation of the intrinsic fluorescence over a large excitation and emission wavelength range for example for tissue diagnosis. Such information, when provided in real time, can be used as a guide to real time optical biopsy in tissue abnormalities diagnostics.

References

1. Yang Y, Celmer EJ, Zurawska-Szczepaniak M, Alfano PR.: Excitation spectrum of malignant and benign breast tissue: A potential optical biopsy approach. Lasers Life Sci.7: 249-265(1996)
2. Landis. S, Murray. T, Bolden. S, Wingo. P: Cancer Statistics, CA-A Cancer Journal for Clinicians. 49: 8-31(1993)
3. Zonios. G, Perelman. L. T. , Backman. V, Manoharan. R, Fitzmaurice. M, Van Dam. J, Feld. M. S: Diffuse reflectance spectroscopy of human adenomatous colon polyps *in vivo.* Appl. Opt. 38 (31): 6628-6637(1999)
4. Richards-Kortum. R and Sevick-Muraca. E: Quantitative optical spectroscopy for tissue diagnosis. Annual Review of Physical Chemistry. 47: 555-606 (1996)
5. Lakowicz. J. R. : *Principles of fluorescence spectroscopy*, 1 ed. Plenum Press, New York, (1983)
6. Itzkan. I, Izatt. J.A: Medical use of lasers. Encyclopedia of Applied Physics. 10: 33-59(1994)
7. Zhang. Q , . Müller. M. G, Wu. J, Feld. M. S: Turbidity-free fluorescence spectroscopy of biological tissue. Optics Letters. 25: 1451-1453 (2000)
8. Wu. J, Feld. M. S, Rava. R.P: Analytical model for extracting intrinsic fluorescence in turbid media. Applied Optics. 32 (19): 3585-3595(1993)
9. Zangaro. R. A , Jr. Silveira. L, Manoharan. R , Zonios. G, Itzkan. I , Dasari. R. R. , Van Dam. J, Feld. M. S: Rapid multiexcitation fluorescence spectroscopy system for *in vivo* tissue diagnosis, Appl. Opt. 35: 5211-5219(1996)
10. Cothren. R. M, Hayes. G. B , Kramer. J. R , Sacks. B. A, Kittrell. C, Feld. M. S: A multifiber catheter with an optical shield for laser angiosurgery. Lasers Life Sci. 1: 1-12(1986)
11. Durkin. A. J, Jaikumar. S, Richards-Kortum. R: Optically dilute, absorbing and turbid

phantoms for fluorescence spectroscopy of homogenous and inhomogenous samples. Applied Spectroscopy. 47 (12): 2114-2121(1993)

12. Brackmann. U: *Lambdachrome laser dyes* ,Lambda Physik GmbH, Goettingen, Germany, (1997)
13. Fishkin. J. B, Coquoz. O, Anderson. E. R , Brenner. M, Tromberg. B. J: Frequency-domain photon migration measurements of normal and malignant tissue optical properties in a human subject. Applied Optics. 36 (1): 10-20(1997)
14. Van Assendelft. O. W: *Spectrophotometry of Haemoglobin Derivatives*, C. C. Thomas, Springfield, IL (1970)
15. Ishimaru. A : *Wave propagation and scattering in random media* , Academic Press, Orlando, FL(1978)
16. Van de Hulst. H. C: *Light Scattering by Small Particles* , Dover Publications, New York(1957)
17. Zonios. G. I. : Diffuse Reflectance Spectroscopy of Human Colon Tissue, Ph. D., Massachusetts Institute of Technology(1998)
18. Zhadin. N. N, Alfano. R. R: Correction of the internal absorption effect in fluorescence emission and excitation spectra from absorbing and highly scattering media: theory and experiment. J. Biomed. Opt. 3 (2): 171-186(1998)
19. Gardner. C. M , Jacques. S. L, Welch. A. J: Fluorescence spectroscopy of tissue: Recovery of intrinsic fluorescence from measured fluorescence. Applied Optics. 35 (10): 1780-1792 (1996)

실시간 광학적 생검에서 형광분광법의 산란과 흡수에 대한 영향

*G.R.Harrison Spectroscopy Lab, Massachusetts Institute of Technology**
아주대학교 †시스템공학과, ‡치료방사선과, §진단방사선과

한승희*,†, Müller M.G.,* 강승희‡, 강해진§

생물학적 조직(Biological Tissue)에서 얻어내는 형광(Fluorescence)은 산란(Scattrering), 흡수(Absorption), 그리고 형광체(Fluorophores)가 원인이 되는, 인트린식 형광(Intrinsic Fluorescence)들에 관한 정보를 갖고 있다. 생물학적 조직의 형광스펙트럼은 조직 내에 존재하는 흡수체(Absorber)와 산란물질(Scatters)들의 영향을 받기 때문에 다른 조직의 생화학적인 인트린식 형광을 선형적인 조합으로 해석할 수 없었다. 생물학적 조직 같은 터비드 매질(Turbid Media)로부터 실험적으로 형광을 얻어서 산란과 흡수의 영향을 조사하기 위하여 본 연구소에서 제작한 장치를 소개하고, 넓은 범위의 흡수체와 산란물질의 농도를 갖고 제작한 조직 팬텀(Tissue Phantom)에 대한 형광과 반사(Reflectance) 스펙트럼을 측정하였다. 형광스펙트럼에 존재하는 산란과 흡수의 왜곡(Distortion)을 제거하기 위하여, 반사스펙트럼에 포함된 산란과 흡수 정보를 이용하는 '광자 이동 모델(Photon Migration Model)'을 적용하였고, 이러한 조직모델에 대한 인트린식 형광을 얻었다. 연구 결과, 모델값과 실제 인트린식 형광 스펙트럼이 훌륭하게 일치함을 확인하였다. 이런 연구를 하게된 동기는, 인간의 조직이 병들어서 진화하면 조직의 생화학적 구성의 변화가 발생하고 이때 인트린식 형광의 변화가 생기기 때문이다. 결론적으로, 조직에 대한 실시간 광학적 생검에서 병든 조직과 정상조직을 단지 형광스펙트럼만으로 구분하는 것은 어렵지만, 인트린식 형광을 이용하면 가능하다.

중심단어: 광학적 생검, 인트린식 형광, 흡수, 산란.